Accepted Manuscript

Physical characterization and fluidization design parameters of wheat germ

Renato D. Gili, R. Martín Torrez Irigoyen, M. Cecilia Penci, Sergio A. Giner, Pablo D. Ribotta

Highlights

Geometrical properties of wheat germ were characterized by image analysis.

Guggenheim-Anderson-de Boer model fits in well the experimental sorption data.

Fluid-dynamic conditions were studied and minimum fluidization velocity was determined.

1 **PHYSICAL CHARACTERIZATION AND FLUIDIZATION DESIGN PARAMETERS OF**

2 **WHEAT GERM.**

3 Renato D. Gili[1], R. Martín Torrez Irigoyen[2], M. Cecilia Penci[1], Sergio A. Giner[2], Pablo D.

4 Ribotta[1, 3]

5 (1) Instituto de Ciencia y Tecnología de Alimentos Córdoba (ICYTAC), CONICET-UNC,

6 Córdoba, Argentina.

7 (2) Centro de Investigación y Criogenia de Alimentos (CIDCA), CONICET-UNLP, Argentina.

8 (3) Instituto Superior de Investigación, Desarrollo y Servicios en Alimentos, Secretaría de

9 Ciencia y Tecnología, UNC, Córdoba, Argentina.

10 **Abstract**

11

12 Wheat germ is the embryo of de wheat seed, it contains a high tocopherol and protein content,

13 and high quality proteins and fatty acids. Also, wheat germ has a considerable enzymatic

14 activity that limits its shelf life. The aims of the study were to physically and sorptionally

15 characterize wheat germ particles, select the more convenient model to describe the

16 relationship between moisture content and water activity of wheat germ and to determine

17 their design parameters of thermal fluidization process with air. The principal axes of the

18 particle were measured by image analysis, and their dimensions and geometric parameters

19 were calculated. Four isotherm models were fitted to experimental data. GAB model was the

20 more accurate to explain the experimental data. The fixed bed density and the void fraction

21 were measured. The fluid-dynamic studies permitted to determine laminar (277.46±17.48)

22 and turbulent (7.79±0.69) coefficients of the Ergun equation and the minimum fluidization

23 velocity (0.35±0.02 m/s).

24

25 **Key words:** Wheat germ; Fluidisation; Sorption isotherm; Physical particle characterization

26

27

28 **Notation**

29

30 A_p Surface area of particle, m^2

31 a_w Water activity

32 C, K, N Coefficients specific to individual equations (Eq. 3 and 4)

33 D Diameter of fluidization chamber, m

34 D_p Effective diameter of particle, m

35 D_e Equivalent diameter of particle, m

36 f_c Coulson factor for wall effect, dimensionless

37 g Average acceleration of gravity, m s^{-2}

38 K_1 Laminar coefficient in Ergun equation

39 K_2 Turbulent coefficient in Ergun equation

40 L_{mf} Height of fluidized bed at the minimum fluidization velocity, m

41 L_0 Fixed bed height, m

42 l_1 Longest axis of wheat germ particle, mm

43 l_2 Intermediate axis of wheat germ particle, mm

44 l_3 Shortest axis of wheat germ particle, mm

45 l_m Average of l_2 and l_3, mm

46 M_a Molar mass of air, kg kmol^{-1}

47 p Atmospheric pressure at sea level, 1.01325 x 10^5 Pa

48 R Gas constant, 8314 J kmol^{-1} K^{-1}

49 s Standard error of the estimate,

50 T_c Temperature, °C

51 T_k Temperature, K

52   V_0 Air superficial velocity, m s^{-1}

53   V_{mf} Minimum fluidization velocity, m s^{-1}

54   V_f Operating fluidization velocity, m s^{-1}

55   V_p Particle volume, m^3

56   W Wheat germ moisture content, kg water/ kg dry matter

57   W_m Monolayer moisture content, dry basis

58   *Greek symbols*

59   π Ratio of a circle's circumference to its diameter (3.14159265…)

60   Δp Static pressure drop across the bed, Pa

61   ε_0 Fixed void fraction, dimensionless

62   ε_{mf} Bed void fraction at minimum the fluidization velocity, dimensionless

63   ρ_p Particle density, kg m^{-3}

64   ρ_{B0} Fixed bed density, kg m^{-3}

65   ρ_a Air density, kg m^{-3}

66   μ_a Air viscosity, kg m^{-1} s^{-1}

67   ψ Sphericity factor, dimensionless

68   **Acronyms**

69

70   GAB   Guggenheim, Anderson and de Boer

71   BET   Brunauer, Emmett and Teller

72   FAIM   Federación Argentina de la Industria Molinera

73   H-T   Henderson-Thompson

74

75

76

77

78

79

1 Introduction

81

Wheat production is an important economic crop in Argentina, of which 14 million tons are produced per year being 5.8 million tons of this wheat ground to obtain wheat flour in 2016 (FAIM, 2017). This industry activity produces a big quantity of wheat germ as a milling by-product. Wheat germ is the embryo of de wheat seed, representing about 2-3 g/100g of the whole grain weight. The germ contains between 8-14 g/100g of oil. (Capitani et al., 2011). Wheat germ contain high quality proteins and fatty acids, a high tocopherol content, vitamins B, dietary fiber, essential amino acids, and functional phytochemicals such as flavonoids and sterols (Marti et al., 2014). Furthermore, the large quantities of wheat flour produced by Argentinian wheat milling industry every year result into an abundant and low cost by-product with an excellent nutritional quality.

Despite of these remarkable nutritional features, wheat germ has a considerable activity due to lipoxygenase and lipase enzymes (Shurpalekar and Rao, 1977). These enzymes deteriorate wheat germ oil quality generating acidity and volatile compounds, which limit wheat germ shelf life to a few days (Sjövall et al., 2000).

Therefore, a process to stabilize the wheat germ has to be devised. Different techniques can be found: application of heat (thermal processes) (Ferrara, et al., 1991; Gili et al., 2017), irradiation (Jha et al., 2013), dehydration processes (Rothe, 1963) or else by chemical preservation, as, for instance by adding some chemical compound as antioxidant (Barnes, 1948) or alkalis (Grandel, 1959). Thermal processes have demonstrated to be effective to stabilize wheat germ, one of these, fluidization, provides an intense heat and mass transfer between material and the hot air, which imply a uniform treatment to the bed being fluidized. (Giner and Calvelo, 1987).

The physical characteristics of wheat germ flakes (low density and non-sticky surface) make it in a suitable material to be stabilized by fluidization.

Yöndem-Makascıoglu et al. (2005) used a spouted bed (a special type of fluidized bed) to stabilize wheat germ. These authors found that a thermal treatment can increase the shelf life of raw wheat germ by a factor of 20 and golden color and pleasant nutty flavor can be imparted by light roasting. However, no mathematical modeling for fluid bed drying of germ

110 was proposed in the literature. A proper model and optimization of the fluidization drying

111 process requires a knowledge of physical characteristics of particles and the fluidization

112 design parameters. Another important tool to model this process and predict the storage

113 conditions are the moisture sorption isotherms at different temperatures. The moisture

114 sorption isotherm of food relates its moisture content (in either desorption or adsorption) to

115 the water activity (a_w) at a definite temperature and it experimentally measured under

116 equilibrium conditions. Several models have been used by researchers to describe the

117 moisture isotherms of food and agricultural materials, as the Brunauer, Emmett and Teller

118 (BET), Guggenheim–Anderson–de Boer (GAB). The latter, has become a widely used

119 expression in food and grain technology, representing an evolution of the classical BET

120 theory of multi-layer adsorption, so physical foundations are clear. The Modified Oswin

121 model and the Modified Henderson or Henderson-Thompson model, are frequently

122 employed to model sorption experimental data (Aviara et al., 2006).

123 Therefore, the objectives of this work were characterize physically and sorptionally wheat

124 germ particles, select the more convenient model to describe the relationship between

125 moisture content and water activity of wheat germ and to determine their design parameters

126 of thermal fluidization process with air.

127 **2   Materials and Methods**

128 **2.1   Material**

129

130 Wheat germ was supplied by local milling industry (JOSE MINETTI Y CIA. LTDA. S.A.C.I,

131 Córdoba, Argentina) after grain milling (2014 harvest).

132

133 **2.2   Preliminary operations**

134

135 Wheat germ was sieved (EJR 2000, Zonytest®) to separate the wheat germ from bran and

136 flour particles, the retention percentage of wheat germ was 93.3±0.3 (g/100 g of wheat

137 germ). The wheat germ particles retained on 20 mesh-size (0.841 mm). In order to reduce

138 enzymatic activity and oil degradation until the heat treatment, the samples were stored at –

139 18°C in a three-layer (polyester, aluminum and polyethylene) package with barriers against

140 oxygen and light until further use (no more than 30 days). Some structural and fluidization

141 properties were analyzed in order to evaluate the possible effect of wheat germ freezing on

142 the laboratory results. No significant changes were found on the major axes of wheat germ

143 particles (measured as described in section 2.5) neither structural changes were detected

144 from the images before and after freezing. Also, no changes in the fluidization pattern and

145 velocity were observed as consequence of the storage of germ at –18°C. Therefore, no

146 significant effect of the frozen storage methodological approach was detected on wheat

147 germ physical properties.

148

2.3 Moisture content

150 Moisture content was determined according to standard method of American Oil Chemistry

151 Society (2009).

152

2.4 Sorption and desorption curves

154

155 The desorption and adsorption equilibrium moisture contents of wheat germ was

156 determined by gravimetric method using a Dynamic Vapour Sorption instrument, model

157 advantage 1 (Surface Measurement Systems Ltd, London, UK) at 24.7 °C and 33.7°C.

158 Briefly, the humidity inside the temperature-controlled chamber was regulated varying the

159 flow of a dry gas (nitrogen) through a humidification stage. The mass changes were

160 measured with a microbalance housed inside of temperature-controlled chamber. Four

161 theoretical models were fitted to the experimental data:

162 1) Guggenheim, Anderson and de Boer (GAB) isotherm equation based on the theory of

163 multi-layer adsorption, has been widely used to describe the sorption behavior of different

164 foods (Giner and Gely, 2005), (Eq. 1).

165
$$W = \frac{W_m \, C \, K_G \, a_w}{(1 - K_G \, a_w)(1 - K_G \, a_w + C \, K_G \, a_w)} \tag{1}$$

166 2) Brunauer, Emmett and Teller (BET) model, it describes the adsorption phenomena at

167 monolayer level.(Aviara et al., 2004), (Eq. 2).

168
$$W = \frac{W_m \, C \, a_w}{(1 - a_w)(1 - a_w + C \, a_w)} \tag{2}$$

169 3) Henderson-Thompson, adopted as one of the standard models the American Society of

170 Agricultural Engineers (ASAE) for the description of the equilibrium moisture content–water

171 activity data of cereals (Eq. 3).

172
$$W = 0.01 \left(- \frac{\ln(1 - a_w)}{K(T + C)} \right)^{\frac{1}{N}} \tag{3}$$

173 4) Modified Oswin, this model includes the temperature dependence and is relatively
174 simple. (Giner and Gely, 2005) Eq.4.

175
$$W = 0.01 \frac{K + C T}{\left(\frac{1}{a_w} - 1 \right)^{\frac{1}{N}}} \tag{4}$$

176 **2.5 Geometric characterization by image analysis**

177

178 The major axes of wheat germ particles were measured by image analysis. The pictures
179 were taken with a Canon Power Shot S70 digital camera mounted on Leica S8 APO
180 magnifying glass using a resolution of 7.1 mega pixels. Two photographs from each wheat
181 germ particle (50 particles) were taken, one with flakes being observed in plan view and
182 another in side view. Each photograph included a circumference with known diameter as
183 reference (0.0006 m). The obtained images were processed using the software ImageJ
184 1.48v (available as freeware from http://rsb.info.nih.gov/ij/).

185 An ellipsoidal geometry was chosen for wheat germ particles. To calculate the particle
186 surface area (A_p) and the particle volume (V_p), the three major axes were used as data to
187 the following formula (Gastón et al., 2002):

188
$$A_p = \frac{\pi}{2} l_1 l_m \left[\frac{l_m}{l_1} + \frac{1}{U} \sin^{-1} U \right] \tag{5}$$

189 where

190
$$U = \frac{(l_1^2 - l_m^2)^{1/2}}{l_1} \tag{6}$$

191
$$l_m = \frac{(l_2 + l_3)}{2} \tag{7}$$

192
$$V_p = \frac{\pi}{6} l_1 l_2 l_3 \tag{8}$$

193 The sphericity factor (ψ) was calculated by de following formula (Torrez Irigoyen and Giner,
194 2011):

195
$$\psi = \frac{\pi D_e^2}{A_p} \tag{9}$$

196 where D_e is the equivalent diameter of wheat germ particle, which represents the diameter
197 of a sphere with the same volume as the wheat germ particle.

198 $$D_p = \psi D_e \tag{10}$$

199 The effective diameter (D_p) represents a diameter of sphere with the same surface-to-

200 volume ratio as that of the wheat germ particle (Torrez Irigoyen and Giner, 2011). The value

201 of D_p is relevant as characteristic particle dimension for the fluid-dynamic studies of fixed

202 beds.

203 **2.6   Particle classification**

204

205 A widely accepted classification for powder particles is that proposed by Geldart (1973),

206 which takes into account two of the more important features of the particles as particle

207 density and size. As a function of these characteristics of the particle, Geldart proposed four

208 groups: A, B, C and D. A powders, exhibit large bed expansion after minimum fluidization

209 and before bubbling; are sometimes termed as slightly cohesive or catalyst type. B powders

210 present bubbling at minimum fluidization velocity with a small bed expansion. C group

211 particles are called cohesive and its powders are difficult to fluidize. D powders are large

212 particles that can form stable spouted beds (Barbosa-Cánovas et al., 2010). Wheat germ

213 particles were classified (taking account of its characteristics) in the Geldart's classification

214 to know the type of fluidization that's should be expected.

215

216 **2.7   Fluidized bed dryer**

217

218 The equipment used (Fig. 1) was a purpose-built fluidized-bed dryer, built in the workshop

219 of the Faculty of Engineering, National University of La Plata, Argentina (Torrez Irigoyen

220 and Giner, 2011). It is made up of (i) a thermally insulated drying chamber, 0.10 m internal

221 diameter and 0.30 m in height with a double glazing inspection window; (ii) hot wire

222 anemometer to record the superficial air velocity through the bed (0- 20 m/s, with an error of

223 0.03 m/s), (iii) a micromanometer Testo 525 (0–25 hPa, with an error of 0.2% at full scale)

224 to measure differences in air pressure across the bed; (iv) a Novus Model N321

225 temperature controller; and (v) a centrifugal fan, powered with a Siemens electric motor

226 (maximum angular speed, 2800 rev/min). Two nickel-plated copper resistance U-shaped, 8

227 mm in diameter each, forms the resistor bank. This resistor bank is capable to heat the air

228 until 325 °C. The Air velocity was controlled through the fan speed, regulated by a

229 frequency inverter WEG Model CFW-08, Brazil.

230

2.8 Determination of fixed bed density and void fraction

232

Fixed bed density was measured in the drying chamber with the wheat germ particles. One hundred grams of wheat germ was weighted (1500 g capacity OHAUS precision balance, readability, 0.01 g) and loaded to the drying chamber. Particles were carried to fluidized condition and then were brought to fixed bed condition again; this step was done in order to standardize bed packing.

The fixed bed height ($L_0 = 0.03 \, m$) was measured (n=3) and fixed bed density (ρ_{B0}) was calculated dividing the wheat germ mass by the bed volume, formed by the volume of particles (understood as envelope volume) plus the voids. The mass of air in the voids was neglected.

The ratio of fixed bed density to the particle density (ρ_p) provides the fraction of the bed occupied by wheat germ particles. Consequently, the fixed bed void fraction (ε_0) was calculated by the following formula:

$$\varepsilon_0 = 1 - \frac{\rho_{B0}}{\rho_p} \qquad (11)$$

246

2.9 Study of the fluid dynamics in fixed and fluidized bed conditions

248

The minimum fluidization velocity (V_{mf}) of wheat germ particles was determined as a parameter based on experimental data. To this end, the pressure drop through the bed, as a function of superficial air velocity, in a range of comprising the fixed bed zone, transition zone between fixed and fluidized states, and the fluidized bed region was measured at 25°C a with the instrument mentioned in Section 2.6.

Fixed bed data were used to determine the two-parameter (K_1 and K_2) of Ergun (1952) expression (Eq. (13)). Then, the V_{mf} value was determined by a mathematical procedure (Torrez Irigoyen and Giner, 2011) from fluidized and fixed states, as is described in the following section.

258

2.10 Determination of parameters of the Ergun equation

The behavior of wheat germ particles into the fluidization chamber was analyzed by the measurement of air pressure drop and of superficial air velocity. The air pressure drops per unit bed height ($\Delta p/L_0(1-\varepsilon_0)$) were plotted as a function of superficial air velocity (V_0).

The Coulson factor (f_c) was used to correct the V_0 (multiplying it by f_c) in the fixed region. This factor takes into account possible wall effects caused by loose bed packing near the chamber walls. (Coulson et al., 1991)

$$f_c = \frac{1}{\left[1 + \frac{\left(\frac{4}{D}\right)}{2\left(\frac{6}{D_a}\right)}\right]^2} \tag{12}$$

For wheat germ particles f_c was 0.993 in consequence, the wall effects for this system was considered low.

For the fixed bed zone, an Ergun type equation (Ergun, 1952) was fitted to the experimental data:

$$\frac{\Delta p}{L_0(1-\varepsilon_0)} = K_1 \frac{(1-\varepsilon_0)\mu_0}{D_p^2 \varepsilon_0^3} V_0 + K_2 \frac{\rho_a}{D_p \varepsilon_0^3} V_0^2 \tag{13}$$

The laminar and turbulent coefficients, K_1 and K_2, were determined for small inorganic particles by Ergun, 1952 as 150 and 1.75, respectively. Delele et al., (2008) suggest that these values depend on product characteristics, particularly in large particles, and must be determined from experimental data fitting the Ergun type equation.

The adequate selection of fixed bed data was carried out in accordance with Torrez Irigoyen and Giner (2011). The Eq. (13) was divided in both members by V_0 in order to express it as a straight line.

$$\frac{\Delta p}{L_0(1-\varepsilon_0)V_0} = K_1 \frac{(1-\varepsilon_0)\mu_0}{D_p^2 \varepsilon_0^3} + K_2 \frac{\rho_a}{D_p \varepsilon_0^3} V_0 \tag{14}$$

Therefore, by reorganizing the experimental data as shown in Eq. (14), and graphing them as function of V_0, the fixed bed zone behavior should be represented by a linear trend. Once the fixed bed data was "isolated", according to Torrez Irigoyen and Giner (2011) the quadratic form (Eq.(13)) was used as this usually provides better fitting than linear version Eq. (14). Fitting to the data was carried out using Statgraphic Centurion XV v 15.1.02, USA. The results of the fitting were obtained by the nonlinear least squares method.

287

2.11 Determination of minimum fluidization velocity

289

290 When the fluid velocity generates a pressure drop through the bed which, when multiplied

291 by the cross sectional area equal the product weight in the fluid, the minimum fluidization

292 velocity (V_{mf}) is reached. The product weight in the fluid was obtained from the difference

293 between product weight and the buoyancy force in the fluid (Werther, 1999). After

294 mathematical operations, the cross sectional area was cancelled out and the mathematical

295 formula becomes:

296
$$\Delta p = (\rho_p - \rho_a)g(1 - \varepsilon_{mf})L_{mf} \tag{15}$$

297 By assuming constant mass from the fixed bed and fluidized bed sides of the minimum

298 fluidization velocity point the next mathematical expression becomes true

299
$$(1 - \varepsilon_{mf})L_{mf} = (1 - \varepsilon_0)L_0 \tag{16}$$

300 By replacing Eq. (16) into Eq. (15) it could be obtained

301
$$\frac{\Delta p}{L_0(1 - \varepsilon_0)} = (\rho_p - \rho_a)g \tag{17}$$

302 Then, the left member of Eq. (17) was replaced by the right member of Eq. (13) evaluated

303 at V_{mf}, in consideration of the fact that V_{mf} nominally belongs to both states, fixed and

304 fluidized states.

305
$$K_2\frac{\rho_a}{D_p\varepsilon_0^3}V_{mf}^2 + K_1\frac{(1 - \varepsilon_0)\mu_0}{D_p^2\varepsilon_0^3}V_{mf} - (\rho_p - \rho_a)g = 0 \tag{18}$$

306 From this formula, V_{mf} is the solution having physical meaning. To obtain this result, the

307 approximation $\varepsilon_{mf} \approx \varepsilon_0$ was employed because the determination of ε_{mf} is cumbersome

308 during the onset of fluidization and the procedure do not usually provide a value reliably

309 different from ε_0. The value of ρ_p was obtained from Kim et al., (2003).

310 Air viscosity (μ_0) and density (ρ_a) were calculated as a function of temperature with the next

311 equations (Formisani et al., 1998).

312
$$\mu_0 = 1.735 \, x \, 10^{-5} + 4.318 \, x \, 10^{-8} T_C \tag{19}$$

313
$$\rho_a = \frac{PM_a}{RT_K} \tag{20}$$

314

315

316

3   Results and discussion

3.1   Sorption and desorption curves

319

Moisture content of wheat germ was 0.1368 ± 0.0015 kg water/ kg of dry matter. DVS
analysis categorized wheat germ as a very hygroscopic class IV material according to
Callahan et al. (1982). The analysis was done at 25°C and 33.7°C, wheat germ presented
an adsorption value of 18.71% (w/w) for 24.7°C and 18.71% (w/w) for 33.7°C at an a_w of
0.80. As this values are higher than 15% (w/w), the European Pharmacopeia classification
is matched with Callahan et al. (1982) classification.

In Figure 2 a sigmoid-shaped isotherm can be observed (type II according to Brunauer et
al., 1940), following a typical sorptional behavior of foods. The adsorption occurs on
nonporous powders or on powders with pore diameters larger than micro pores. The
inflection point or knee of the isotherms, as was expected, occurs near the completion of
the first adsorbed monolayer and with increasing relative pressure. (Lowell and Shields,
1984) This point was found at a water activity values close to 0.4.

The desorption curve was observed to be slightly above the adsorption curve showing
therefore some hysteresis. This phenomenon was observed for a_w values between 0 and
0.5 at 25°C and between 0 and 0.25 at 33.7°C. Hysteresis has been related to the nature
and state of the components in a food, reflecting their potential for structural and
conformational rearrangements (Yogendrarajah et al., 2015).

As was mentioned previously, wheat germ presented a high enzymatic activity. The lipase
of wheat has an optimal water activity of 0.87 according to Rose and Pike, (2006). Raw
wheat germ had a moisture content of 0.1368 kg water per 1 kg of dry matter, this represent
a water activity slightly above 0.7. At this level of water activity, the wheat germ presented a
strong activity of lipase and lipoxygenase enzymes and it is possible that, with extended
storage time, some microorganisms can grow. For most foods, the critical water activity
zone (where microorganisms begin to grow) is 0.6-0.7 (Durance, 2002). For these reasons
is advisable to store wheat germ in a 0.4-0.5 water activity range or, using the isotherm
data, at moisture contents between 5 to 8 % (d.b.).

346 Four sorption models, named and described previously in section 2.4, were fitted to the

347 experimental data. The fitted parameters from Eq.1 and Eq.2 were presented in Table 1,

348 and the fitted parameters from Eq. 3 and Eq. 4 were listed in Table 2. In both tables, the

349 asymptotic standard error (ASE) of parameters are included in parentheses.

350 Adopting the coefficient of determination r^2 as a criterion to pre-select sorption equations,

351 BET, GAB, modified Oswin and Henderson-Thompson (H-T) were found to be acceptable

352 to reproduce the experimental isotherms for the wheat germ ($r^2 > 0.9$). Comparing GAB and

353 BET monolayer value (W_m), the GAB value was approximately 22% higher than the BET at

354 24.7°C and approximately 20% higher at 33.7°C, which is in agreement with Timmermann

355 et al. (2001) to several foods and foodstuffs.

356 It is important to highlight that the BET isotherm only explain the 0.01-0.50 range of a_w

357 (Durance, 2002). This narrow range limits the applicability of this model so it was not

358 considered appropriate to describe the adsorption phenomena in wheat germ.

359 Nevertheless, by analyzed the standard errors of the estimate (s), the GAB model becomes

360 slightly more accurate with a value for s of 0.0022 decimal moisture content, d.b. at 24.7°C

361 and 0.0021 decimal moisture content, d.b. at 33.7°C. This methodology of model selection

362 was applied by Giner and Gely (2005). Henderson-Thompson and Modified Oswin, in spite

363 of their simplicity, are acceptable for predicting the equilibrium moisture content of wheat

364 germ, similar results for this models were published for soya bean and sunflower seeds by

365 Aviara et al. (2004) and Giner and Gely (2005), respectively.

366 The behavior of fitted models is observed in Fig. 3, the equilibrium moisture content is

367 compared at 25°C and 33.7°C with predictions by four isotherm models.

368

369 **3.2 Geometric characterization by image analysis**

370

371 A total of 50 particles of wheat germ were measured by image analysis. The three mayor

372 axes were determined by considering the circular standard reference in the image (Fig. 4).

373 Table 3 shows the measures values of main axes, and the calculated values of surface

374 area, particle volume, equivalent spherical diameter and effective diameter (Eq. 5 to 10).

375

3.3 Particle classification

According to wheat germ density (1234.23 kg/m^3) and size particle (0.623 mm) it is the limit region between group A and B, but according to the observed particle behavior during fluidization, wheat germ belongs to group B of Geldart's classification, since a bubbling at minimum fluidization velocity with a small bed expansion was observed.

3.4 Determination of Ergun parameters

The bed pressure drop per unit bed height was plotted as a function of superficial air velocity for wheat germ. At low velocities, an increasing slope and concave shape of the curve was observed, being this behavior comparable with that reported by other authors (Torrez Irigoyen and Giner, 2011 and Sau et al., 2007) which is a characteristic behavior of the fixed bed region. At higher velocities, as was expected for the fluidized region, the curve became horizontal.

The fixed bed zone was determined by arranging the experimental data as indicated by the left member of Eq. (14) as function of V_0. The fixed bed zone is characterized by a regular behavior, for this particle, this behavior pattern was presented up to 0.26 m/s after that, the observed behavior became irregular or transitional. Using this procedure, the fixed bed region was delimited in the velocity range of 0.05 - 0.26 m/s.

Once delimited the pure fixed bed zone, experimental data were utilized as indicated by the left member of Eq. (13) as a function of V_0 and then, the parabolic form of Ergun model (Eq. (13)) was fitted to these data using the bed void fraction and effective diameter of Table 4. The parameters obtained (K_1 and K_2) were 277.46 (17.48) and 7.79 (0.69) respectively, the corresponding ASE is between parenthesis. The corrected coefficient of determination (r^2) was 0.994.

As mentioned previously in section 2.9, K_1 and K_2 depend on particle characteristics, mainly surface roughness, size and shape (Escardino et al., 1974). The values obtained were higher than those reported by Torrez Irigoyen and Giner, 2011 for soybean grains. The value of K_1 determined here was lower than the obtained by Escardino et al., 1974 for wheat grains, while K_2 was greater than the corresponding value. This can be related to particle shape, the wheat germ particle is small and plane. These characteristics may have

408 influenced the bed packing into the drying chamber, creating sharp changes in the direction

409 of the air flow when percolating through the bed (Yang, 2003). Furthermore, wheat germ

410 has a rough particle surface and this characteristic have also contributed to the large values

411 of K_1 and K_2.

412 This has been in agreement with Molenda et al., (2005) who informed that the non-spherical

413 shape of grains and random size distribution resulted in coefficients K_1 and K_2 being

414 considerably greater than the theoretical values for spherical particles. This is in

415 concordance with the results obtained in this work.

416 The predicted lines and experimental pressure drops (symbols) were plotted as a function

417 of superficial air velocity using the parameters obtained from fitted Ergun equation (Fig. 5).

418 The agreement of experimental and predicted values was satisfactory for the wheat germ

419 particles.

420

421 **3.5   Determination of V_{mf}**

422

423 The minimum fluidization velocity was obtained from Eq. (18) using the measured particle

424 data (D_p, ε_0). After solving the Eq. (18), the V_{mf} for wheat germ particles fluidized in air at

425 ~25 °C was 0.35±0.02 m/s. This minimum fluidization velocity, in the dryer utilized,

426 correspond to 0.003 m³/s approximately. This flow is very lower than the 0.011 m³/s

427 informed by Yöndem-Makascıoğlu et al. (2005) to stabilize wheat germ in a spouted

428 fluidized bed.

429

430 **4   Conclusion**

431

432 In the present investigation, some geometrical properties (V_p, A_p, ψ, D_p, D_e) of wheat germ

433 were characterized by image analysis. The wheat germ particle was classified as group B of

434 Geldart's classification.

435 Four isotherm models were fitted to experimental sorption data, GAB model resulted the

436 most accurate to explain the experimental behavior. The monolayer moisture content given

437 by the GAB model was 0.050 ± 0.002 kg water per kg dry matter at 24.7°C and 0.055 ±

438 0.002 kg water per kg dry matter at 33.7°C. Wheat germ may be storage at a water activity

439 of 0.4-0.5 (5-8% of moisture content) to avoid spoilage factors as enzymatic activity, lipid

440 quality losses and microorganism growth.

441 The fixed bed density and the void fraction were measured. The fluid-dynamic

442 characteristics of wheat germ in fixed bed was studied, the laminar and turbulent (K_1 and

443 K_2) parameters of Ergun equation were fitted to the data and the minimum fluidization

444 velocity of wheat germ determined at 25°C to be 0.35±0.02 m/s.

445

5   Acknowledgments

447

452

6   Bibliography

AOCS (2009) Official methods and recommended practices of the American Oil Chemists'
Society (5th ed.). Champaign, Illinois, USA.

Aviara, N.A., Ajibola, O.O., Aregbesola, O.A., Adedeji, M.A., 2006. Moisture sorption
isotherms of sorghum malt at 40 and 50 °C. J. Stored Prod. Res. 42, 290–301.
doi:10.1016/j.jspr.2005.05.001

Aviara, N.A., Ajibola, O.O., Oni, S.A., 2004. Sorption Equilibrium and Thermodynamic
Characteristics of Soya Bean. Biosyst. Eng. 87, 179–190.
doi:10.1016/j.biosystemseng.2003.11.006

Barbosa-Cánovas, G. V., Ortega-Rivas, E., Juliano, P., Yan, H., 2010. Food Powders
Physical Properties, Processing, and Functionality. Annu. Rev. Food Sci. Technol. 1,
211–239. doi:10.1146/annurev.food.102308.124155

Barnes, H.M., 1948. Process of stabilizing organic materials and products of said process.
US 2448208 A.

Brunauer, S., Deming, L.S., Deming, W.E., Teller, E., 1940. On a Theory of the van der
Waals Adsorption of Gases. J. Am. Chem. Soc. 62, 1723–1732.
doi:10.1021/ja01864a025

Callahan, J.C., Cleary, G.W., Elefant, M., Kaplan, G., Kensler, T., Nash, R.A., 1982.
Equilibrium Moisture Content of Pharmaceutical Excipients. Drug Dev. Ind. Pharm. 8,
355–369. doi:10.3109/03639048209022105

Capitani, M., Mateo, C.M., Nolasco, S.M., 2011. Effect of temperature and storage time of
wheat germ on the oil tocopherol concentration. Brazilian J. Chem. Eng. 28, 243–250.

Coulson, J.M., Richardson, J.F., Harker, J.H., Backhurst, J.., 1991. Chemical Engineering
Volume 2: Particle Technology and Separation Processes, 5th ed, Chemical
Engineering Science. Butterworth-Heinemann, Oxford. doi:10.1016/0009-
2509(60)80030-9

Delele, M.A., Tijskens, E., Atalay, Y.T., Ho, Q.T., Ramon, H., Nicolaï, B.M., Verboven, P.,
2008. Combined discrete element and CFD modelling of airflow through random
stacking of horticultural products in vented boxes. J. Food Eng. 89, 33–41.
doi:10.1016/j.jfoodeng.2008.03.026

484   Durance, T., 2002. Handbook of Food Preservation. Food Res. Int. 35, 409.
485   doi:10.1016/S0963-9969(00)00143-5

486   Ergun, S., 1952. Fluid Flow Through Packed Columns. Chem. Eng. Prog. 48, 89–94.

487   Escardino, A., Ruiz, F., Barbero, P., 1974. Circulación de aire a través de lechos formados
488   por granos de cereales. Rev. Agroquímica y Tecnol. Aliment. 10, 528–539.

489   FAIM, 2017. Molienda y producción de Harina [WWW Document]. URL
490   http://www.faim.org.ar/Nacional.aspx (accessed 2.14.17).

491   Ferrara P.J., Ridge R.D., & Benson, J.., 1991. Method of producing shelf stable wheat
492   germ. US Pat 5.063.079.

493   Formisani, B., Girimonte, R., Mancuso, L., 1998. Analysis of the fluidization process of
494   particle beds at high temperature. Chem. Eng. Sci. 53, 951–961. doi:10.1016/S0009-
495   2509(97)00370-9

496   Gastón, A.L., Abalone, R.M., Giner, S. a., 2002. Wheat drying kinetics. Diffusivities for
497   sphere and ellipsoid by finite elements. J. Food Eng. 52, 313–322. doi:10.1016/S0260-
498   8774(01)00121-2

499   Geldart, D., 1973. Types of gas fluidization. Powder Technol. 7, 285–292.
500   doi:10.1016/0032-5910(73)80037-3

501   Gili, R.D., Palavecino, P.M., Cecilia Penci, M., Martinez, M.L., Ribotta, P.D., 2017. Wheat
502   germ stabilization by infrared radiation. J. Food Sci. Technol. 54, 71–81.
503   doi:10.1007/s13197-016-2437-z

504   Giner, S.A., Gely, M.C., 2005. Sorptional parameters of sunflower seeds of use in drying
505   and storage stability studies. Biosyst. Eng. 92, 217–227.
506   doi:10.1016/j.biosystemseng.2005.06.002

507   Giner, S. A., Calvelo, A., 1987. Modelling of wheat drying in fluidized beds. J. Food Sci. 52,
508   1358–1363. doi:10.1111/j.1365-2621.1987.tb14082.x

509   Grandel, F., 1959. Process of making germ flakes. US Pat 2879167 A.

510   Jha, P.K., Kudachikar, V.B., Kumar, S., 2013. Lipase inactivation in wheat germ by gamma
511   irradiation. Radiat. Phys. Chem. 86, 136–139. doi:10.1016/j.radphyschem.2013.01.018

512   Kim, Y.S., Flores, R.A., Chung, O.K., Bechtel, D.B., 2003. Physical, chemical, and thermal
513   characterization of wheat flour milling coproducts. J. Food Process Eng. 26, 469–488.

514   doi:10.1111/j.1745-4530.2003.tb00613.x

515 Lowell, S., Shields, J.E., 1984. Powder Surface Area and Porosity, Statewide Agricultural
516   Land Use Baseline 2015. Springer Netherlands, Dordrecht. doi:10.1007/978-94-009-
517   5562-2

518 Marti, A., Torri, L., Casiraghi, M.C., Franzetti, L., Limbo, S., Morandin, F., Quaglia, L.,
519   Pagani, M.A., 2014. Wheat germ stabilization by heat-treatment or sourdough
520   fermentation: effects on dough rheology and bread properties. LWT - Food Sci.
521   Technol. doi:10.1016/j.lwt.2014.06.039

522 Molenda, M., Montross, M.D., Mcneill, S.G., Horabik, J., 2005. Airflow resistance of seeds
523   at different bulk densities using Ergun's equation. Trans. ASAE 48, 1137–1145.

524 Rose, D.J., Pike, O. A., 2006. A simple method to measure lipase activity in wheat and
525   wheat bran as an estimation of storage quality. JAOCS, J. Am. Oil Chem. Soc. 83,
526   415–419. doi:10.1007/s11746-006-1220-0

527 Rothe, M., 1963. Uber ein neues Stabilisierungsverfahren fur Weizenkeime. Mol. Nutr. Food
528   Res. 7, 579–587. doi:10.1002/food.19630070805

529 Sau, D.C., Mohanty, S., Biswal, K.C., 2007. Minimum fluidization velocities and maximum
530   bed pressure drops for gas–solid tapered fluidized beds. Chem. Eng. J. 132, 151–157.
531   doi:10.1016/j.cej.2007.01.036

532 Shurpalekar, S.R., Rao, P.H., 1977. Wheat Germ. Adv. Food Res. 23, 187–304.

533 Sjövall, O., Virtalaine, T., Lapveteläinen, a, Kallio, H., 2000. Development of rancidity in
534   wheat germ analyzed by headspace gas chromatography and sensory analysis. J.
535   Agric. Food Chem. 48, 3522–7.

536 Timmermann, E.O., Chirife, J., Iglesias, H.A., 2001. Water sorption isotherms of foods and
537   foodstuffs: BET or GAB parameters? J. Food Eng. 48, 19–31. doi:10.1016/S0260-
538   8774(00)00139-4

539 Torrez Irigoyen, R.M., Giner, S. a., 2011. Fluidisation velocities during processing of whole
540   soybean snack. J. Food Eng. 107, 90–98. doi:10.1016/j.jfoodeng.2011.05.040

541 Werther, J., 1999. Measurement techniques in fluidized beds. Powder Technol. 102, 15–36.

542 Yang, W. C., 2003. Handbook of fluidization and fluid-particle systems. China Particuology
543   1, 137. doi:10.1016/S1672-2515(07)60126-2

544 Yogendrarajah, P., Samapundo, S., Devlieghere, F., De Saeger, S., De Meulenaer, B.,

545   2015. Moisture sorption isotherms and thermodynamic properties of whole black

546   peppercorns (Piper nigrum L.). LWT - Food Sci. Technol. 64, 177–188.

547   doi:10.1016/j.lwt.2015.05.045

548 Yöndem-Makascioğlu, F., Gürün, B., Dik, T., Kincal, N.S., 2005. Use of a spouted bed to

549   improve the storage stability of wheat germ followed in paper and polyethlyene

550   packages. J. Sci. Food Agric. 85, 1329–1336. doi:10.1002/jsfa.2102

551

Figure 1. (A) Thermally insulated drying chamber with double glazing for inspection. (B) Micromanometer Testo 525. (C) Temperature controller Novus Model N321. (D) Velocity controller. (E) Hot wire digital anemometer Testo 425. (F) Centrifugal fan.
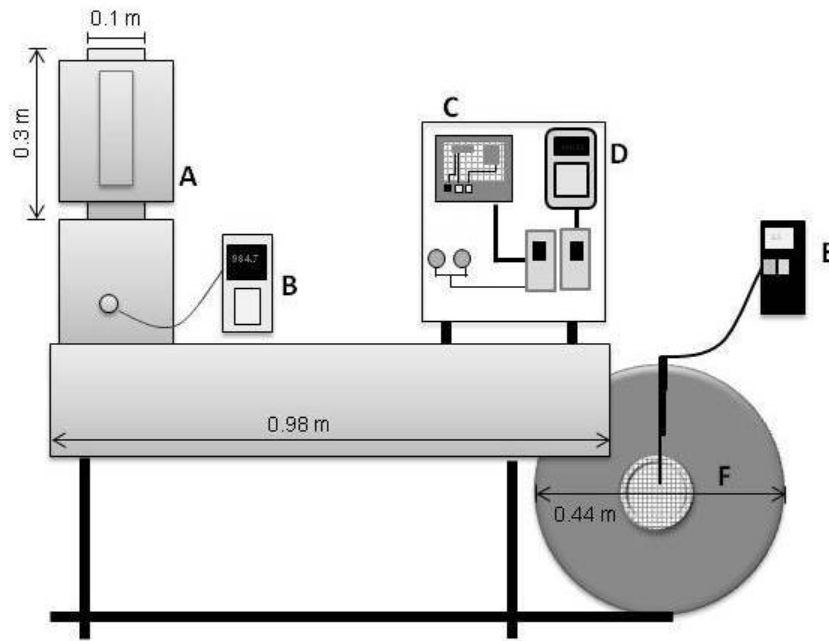
Figure 2. Sorption and desorption curves of wheat germ particle at 25°C and 35 °C.
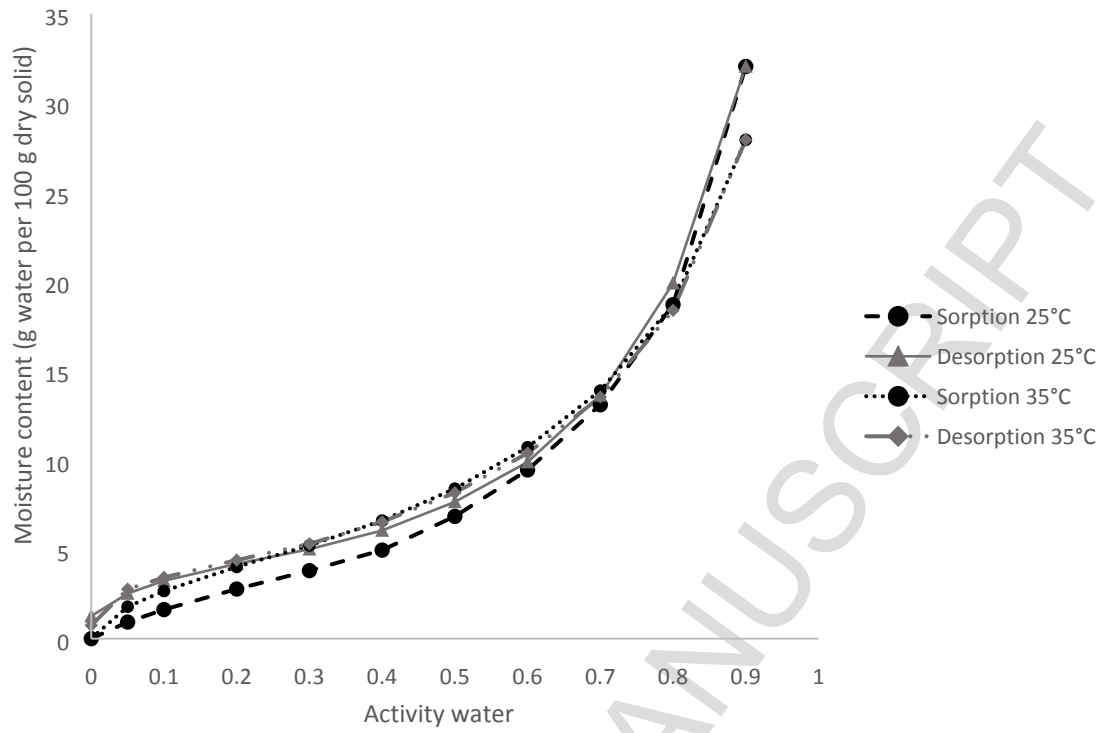
Figure 3. Experimental moisture content of wheat germ particles (d.b.) as a function of water activity at 25 °C (▲) and 33.7 °C (○). Experimental and predicted values for each sorption model. a) Henderson-Thompson (H-T); b) GAB; c) Modified oswin and d) BET

(a)

(b)

(c)

(d)

Figure 4. Plan view of wheat germ particle with l_1 and l_2 mayor axes and circular reference point.
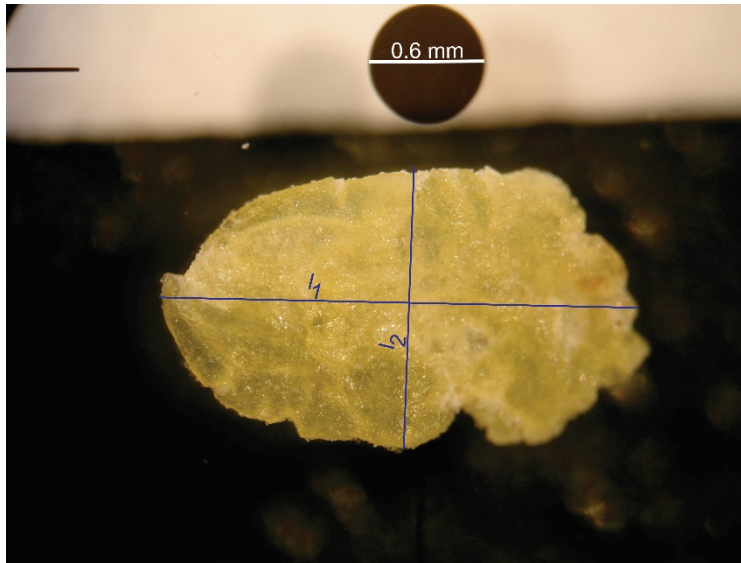
Figure 5. Bed pressure drop per unit bed height as a function of superficial air velocity. Experimental (▲) and Ergun-predicted values (⋯).

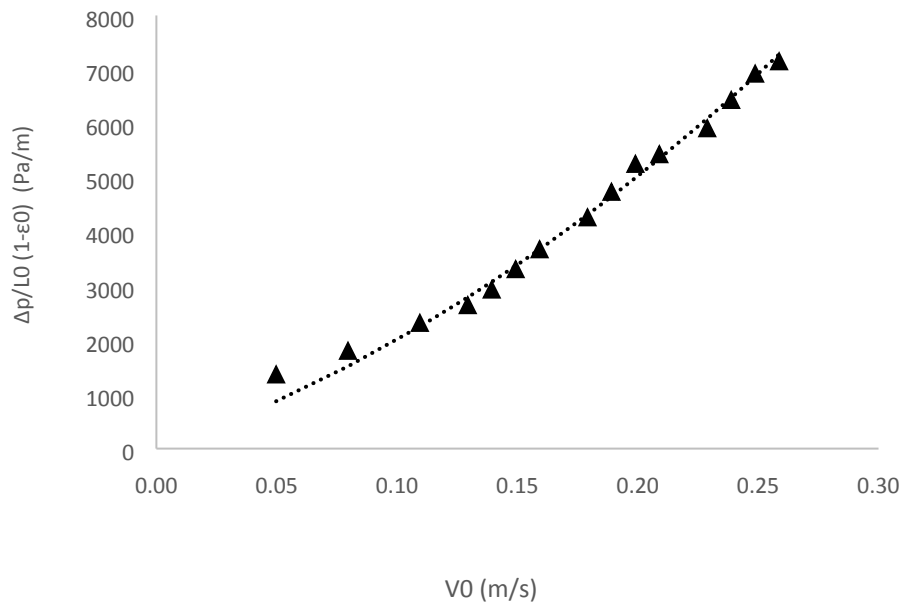**Table 1**. Parameters determined by fitting the GAB and BET model at the two analyzed temperatures.

	Temperature (°C)	W_m	K_G	C	r^2	s
BET	25	0.041 (0.001)	-	4.780 (0.560)	0.9963	0.0013
	35	0.046 (0.001)	-	10.068 (0.654)	0.9986	0.0009
GAB	25	0.050 (0.002)	0.945 (0.005)	3.098 (0.353)	0.9995	0.0022
	35	0.055 (0.001)	0.900 (0.005)	7.098 (0.726)	0.9994	0.0021

*BET $0.05 < a_w < 0.50$

Table 2. Parameters determined by fitting the Henderson-Thompson and Oswin Modified models at the two analyzed temperatures.

	Temperature (°C)	K	C	N	r^2	s
H-T	25	0.0062 (0.0001)	0.175 (0.001)	0.785 (0.002)	0.9918	0.0087
	35	0.0117(0.0003)	-27.745 (0.0001)	1.060 (0.001)	0.9891	0.0087
Oswin modified	25	0.035 (0.043)	0.286 (0.001)	1.454 (0.001)	0.9992	0.0027
	35	-105.15 (0.06)	3.376(0.00001)	1.850(0.001)	0.9989	0.0028

Table 3. Wheat germ properties determined by image analysis and calculated.

	Mean	Min	Max	Unit
l_1	2.28	1.65	3.39	mm
l_2	1.59	1.19	2.13	mm
l_3	0.29	0.17	0.41	mm
A_p	5.26	3.65	9.21	mm^2
V_p	0.49	0.24	0.97	mm^3
D_e	0.969	0.766	1.223	mm
D_p	0.623	0.366	0.849	mm
ψ	0.62	0.477	0.79	Dimensionless

n=50

Table 4. Fixed bed properties determined

ρ_p	1234.23	kg/m^3
ρ_{B0}	413.83	kg/m^3
L_0	0.03	m
ε_0	0.664	Dimensionless